Available online at www.sciencedirect.com
ScienceDirect
Journal of Solid State Chemistry 181 (2008) 878–883
JOURNAL OF SOLID STATE CHEMISTRY
www.elsevier.com/locate/jssc

Rare earth–nickel–indides $Dy_5Ni_2In_4$ and $RE_4Ni_{11}In_{20}$ (RE = Gd, Tb, Dy)

Yuriy B. Tyvanchuk[a,b], Ute Ch. Rodewald[b], Yaroslav M. Kalychak[a], Rainer Pöttgen[a,*]

[a]*Inorganic Chemistry Department, Ivan Franko National University of Lviv, Kyryla and Mephodiya Street 6, 79005 Lviv, Ukraine*
[b]*Institut für Anorganische und Analytische Chemie, Universität Münster, Corrensstrasse 30, 48149 Münster, Germany*

Received 13 December 2007; received in revised form 21 January 2008; accepted 26 January 2008
Available online 6 February 2008

Abstract

The new rare earth metal (RE)–nickel–indides $Dy_5Ni_2In_4$ and $RE_4Ni_{11}In_{20}$ (RE = Gd, Tb, Dy) were synthesized from the elements by arc-melting. Well-shaped single crystals were obtained by special annealing sequences. The four indides were investigated by X-ray diffraction on powders and single crystals: $Lu_5Ni_2In_4$ type, *Pbam*, $Z = 2$, $a = 1784.2(8)$, $b = 787.7(3)$, $c = 359.9(1)$ pm, w$R_2 = 0.0458$, 891 F^2 values, 36 variables for $Dy_5Ni_2In_4$, $U_4Ni_{11}Ga_{20}$ type, $C2/m$, $a = 2254.0(9)$, $b = 433.8(3)$, $c = 1658.5(8)$ pm, $\beta = 124.59(2)^\circ$, w$R_2 = 0.0794$, 2154 F^2 values, 108 variables for $Gd_4Ni_{11}In_{20}$, $a = 2249.9(8)$, $b = 432.2(1)$, $c = 1657.9(5)$ pm, $\beta = 124.59(2)^\circ$, w$R_2 = 0.0417$, 2147 F^2 values, 108 variables for $Tb_4Ni_{11}In_{20}$, and $a = 2252.2(5)$, $b = 430.6(1)$, $c = 1659.7(5)$ pm, $\beta = 124.58(2)^\circ$, w$R_2 = 0.0550$, 2003 F^2 values, 109 variables for $Dy_4Ni_{10.80}In_{20.20}$. The 2*d* site in the dysprosium compound shows mixed Ni/In occupancy. Most nickel atoms in both series of compounds exhibit trigonal prismatic coordination by indium and rare earth atoms. Additionally, in the $RE_4Ni_{11}In_{20}$ compounds one observes one-dimensional nickel clusters (259 pm Ni_1–Ni_6 in $Dy_4Ni_{10.80}In_{20.20}$) that are embedded in an indium matrix. While only one short In_1–In_2 contact at 324 pm is observed in $Dy_5Ni_2In_4$, the more indium-rich $Dy_4Ni_{10.80}In_{20.20}$ structure exhibits a broader range in In–In interactions (291–364 pm). Together the nickel and indium atoms build up polyanionic networks, a two-dimensional one in $Dy_5Ni_2In_4$ and a complex three-dimensional network in $Dy_4Ni_{10.80}In_{20.20}$. These features have a clear consequence on the dysprosium coordination, i.e. a variety of short Dy–Dy contacts (338–379 pm) in $Dy_5Ni_2In_4$, while the dysprosium atoms are well separated (430 pm shortest Dy–Dy distance) within the distorted hexagonal channels of the $[Ni_{10.80}In_{20.20}]$ polyanion of $Dy_4Ni_{10.80}In_{20.20}$. The crystal chemistry of both structure types is comparatively discussed.

Keywords: Indium; Intermetallics; Crystal chemistry

1. Introduction

Intermetallic rare earths (RE)–nickel–indides have attracted broad interest in recent years with respect to their interesting crystal chemistry and their greatly varying magnetic properties. An overview has been given in a recent review article [1]. To give some examples, GdNiIn is a ferromagnet with a comparatively high-Curie temperature of 83 K [2,3]. The valence fluctuating system CeNiIn [4] shows a switch to a ferromagnetically ordered state ($T_C = 6.8$ K) in $CeNiInH_{1.8}$ [5] upon hydrogenation and $Ce_5Ni_6In_{11}$ [6,7] is a heavy fermion material with two crystallographically independent cerium sites which show antiferromagnetic ordering at $T_{N1} = 1.10$ and $T_{N2} = 0.63$ K. $CeNiIn_2$ [8] orders ferro- or ferrimagnetically at 3.4 K.

Most of the $RE_xNi_yIn_z$ compounds are easily accessible in polycrystalline form via simple arc-melting under argon. For determination of the complex crystal structures, small single crystals are required. The latter can be grown by flux techniques or via special thermal annealing sequences. This has been successfully achieved for the indides $YNiIn_2$, $Y_4Ni_{11}In_{20}$ [9], HT-$GdNiIn_2$ [10], the series $RE_{10}Ni_{9+x}In_{20}$ [11] and $RE_{14}Ni_3In_3$ [12]. We have continued our phase analytical investigations in the RE–Ni–In systems. Herein, we report on the crystal growth and structure refinements of new indides $Dy_5Ni_2In_4$ ($Lu_5Ni_2In_4$ type [13])

*Corresponding author. Fax: +49 251 83 36002.
E-mail addresses: yutyv@franko.lviv.ua (Y.B. Tyvanchuk), pottgen@uni-muenster.de (R. Pöttgen).

0022-4596/$ - see front matter © 2008 Elsevier Inc. All rights reserved.
doi:10.1016/j.jssc.2008.01.035

and $RE_4Ni_{11}In_{20}$ (RE = Gd, Tb, Dy) with $U_4Ni_{11}Ga_{20}$ type [14].

2. Experimental

2.1. Synthesis

Starting materials for the preparation of the $Dy_5Ni_2In_4$ and $RE_4Ni_{11}In_{20}$ samples were sublimed ingots of the rare earth elements (Johnson Matthey, Chempur or Kelpin), nickel wire (Johnson Matthey, ∅ 0.38 mm), and indium tear drops (Heraeus), all with stated purities better than 99.9%. Pieces of the rare earth elements were first arc-melted [15] under argon to small buttons. The argon was purified with titanium sponge (900 K), silica gel, and molecular sieves. This pre-melting procedure prevents shattering during the subsequent exothermic reactions. The rare earth buttons were subsequently mixed with pieces of the nickel wire and the indium tear drops in the ideal 5:2:4 and 4:11:20 atomic ratios and arc-melted three times to ensure homogeneity. The total weight loss after the melting procedures was always smaller that 0.5%.

After the arc-melting procedure, X-ray pure $Dy_5Ni_2In_4$ and the $RE_4Ni_{11}In_{20}$ samples were obtained only as polycrystalline powders. Special heat treatment was necessary for the growth of single crystals. The samples were powdered and cold-pressed to small pellets (6 mm diameter). The pellets were then put in tantalum containers that have been sealed in evacuated silica tubes as an oxidation protection. The samples were first heated at 1270 K within 5 h and held at that temperature for 4 h. Subsequently the temperature was lowered at a rate of 5 K/h to 1020 K, then at a rate of 17.5 K/h to 870 K, and finally cooled to room temperature within 5 h. After cooling to room temperature, the samples could easily be separated from the tantalum crucibles by pounding at their base. No reaction of the samples with the crucibles could be detected. All samples are brittle and stable in air over several weeks. Single crystals exhibit metallic luster.

2.2. Single crystal X-ray diffraction

Irregularly shaped crystals of $Dy_5Ni_2In_4$ and well-shaped crystals of $RE_4Ni_{11}In_{20}$ were selected from the crushed annealed samples. The crystals were glued to small quartz fibres using bees wax. The crystal quality was checked by Laue photographs on a Buerger camera, equipped with the same Fujifilm, BAS-1800 imaging plate. Intensity data of the $Dy_5Ni_2In_4$ and $Dy_4Ni_{10.80}In_{20.20}$ crystals were collected on a Stoe IPDS II diffractometer (graphite monochromatized Mo $K\alpha$ radiation) in oscillation mode. Numerical absorption corrections were applied to the data sets. The $Gd_4Ni_{11}In_{20}$ and $Tb_4Ni_{11}In_{20}$ crystals were measured at room temperature by use of a four-circle diffractometer (CAD4) with graphite monochromatized Mo $K\alpha$ (71.073 pm) radiation and a scintillation counter with pulse height discrimination. Scans were taken in the $\omega/2\theta$ mode. An empirical absorption correction was applied on the basis of Ψ-scan data, followed by a spherical absorption correction. Relevant crystallographic data for the data collections and evaluations are listed in Table 1.

2.3. X-ray powder data

$Dy_5Ni_2In_4$ and the $RE_4Ni_{11}In_{20}$ samples were characterized through Guinier powder patterns using Cu $K\alpha_1$ radiation and α-quartz ($a = 491.30$, $c = 540.46$ pm) as an internal standard. The Guinier camera was equipped with an imaging plate system (Fujifilm, BAS-1800). The orthorhombic and monoclinic lattice parameters (Table 1) were determined from least-squares calculations. To ensure proper indexing, the experimental patterns were compared with calculated ones [16], taking the atomic positions obtained from the structure refinements of the dysprosium compounds.

2.4. Scanning electron microscopy

The $Dy_5Ni_2In_4$ and $RE_4Ni_{11}In_{20}$ single crystals investigated on the diffractometer were analysed using a LEICA 420 I scanning electron microscope with the rare earth trifluorides, nickel, and indium arsenide as standards (20 kV acceleration voltage; 5 min counting time on ten points for each crystal). No impurity elements heavier than sodium (detection limit of the instrument) were observed. The compositions determined semiquantitatively by EDX were close to the ideal compositions.

3. Results and discussion

3.1. Structure refinements

The IDPS data set of the $Dy_5Ni_2In_4$ crystal showed a primitive orthorhombic lattice and the systematic extinctions were compatible with space group *Pbam*, in agreement with our previous investigations on $Sc_5Ni_2In_4$ [17]. The $RE_4Ni_{11}In_{20}$ crystals showed monoclinic cells and only the extinctions of a C-centered lattice, leading to space groups $C2/m$, Cm, and $C2$, of which the centrosymmetric group was found to be correct during the structure refinements, in good agreement with the previous data on $Y_4Ni_{11}In_{20}$ [9]. Subsequently, the atomic positions of $Sc_5Ni_2In_4$ [17] and $Y_4Ni_{11}In_{20}$ [9] were taken as starting values and the structures were refined with anisotropic displacement parameters for all atoms with SHELXL-97 (full-matrix least-squares on F_o^2) [18]. The occupancy parameters were refined in separate series of least-squares cycles as a check for the correct site assignment. The $Dy_5Ni_2In_4$, $Gd_4Ni_{11}In_{20}$, and $Tb_4Ni_{11}In_{20}$ crystals revealed full occupancy for all sites and in the final cycles the ideal occupancy parameters were assumed again.

Most sites of the $Dy_4Ni_{11}In_{20}$ crystal also revealed full occupancy, however, similar to the $RE_4Pd_{10}In_{21}$ [19] and $RE_4Pt_{10}In_{21}$ [20] series, the 2*d* site revealed

Table 1
Crystal data and structure refinement for $Dy_5Ni_2In_4$, $Gd_4Ni_{11}In_{20}$, $Tb_4Ni_{11}In_{20}$ and $Dy_4Ni_{10.80(3)}In_{20.20(3)}$

Empirical formula	$Dy_5Ni_2In_4$	$Gd_4Ni_{11}In_{20}$	$Tb_4Ni_{11}In_{20}$	$Dy_4Ni_{10.80(3)}In_{20.20(3)}$
Structure type	$Lu_5Ni_2In_4$	$U_4Ni_{11}Ga_{20}$	$U_4Ni_{11}Ga_{20}$	$U_4Ni_{11}Ga_{20}$
Molar mass (g/mol)	1389.20	3571.21	3577.89	3603.43
Space group	*Pbam*	*C*2/*m*	*C*2/*m*	*C*2/*m*
Z	2	2	2	2
Unit cell dimensions (Guinier powder data)				
a (pm)	1784.2(8)	2254.0(9)	2249.9(8)	2252.2(5)
b (pm)	787.7(3)	433.8(3)	432.2(1)	430.6(1)
c (pm)	359.9(1)	1658.5(8)	1657.9(5)	1659.7(5)
β (deg)		124.59(2)	124.59(2)	124.58(2)
V (nm^3)	0.5059	1.3350	1.3272	1.3252
Calculated density (g/cm^3)	9.12	8.88	8.95	9.03
Crystal size (μm^3)	$20\times40\times60$	$20\times20\times260$	$20\times20\times130$	$20\times20\times150$
Detector distance (mm)	90	–	–	80
Exposure time (min)	6	–	–	1
ω range; increment (deg)	0–180, 1.0	–	–	0–180, 1.0
Absorption coefficient (mm^{-1})	48.9	34.2	35.0	35.7
Integr. param. *A*, *B*, EMS	13.0, 3.0, 0.012	–	–	13.0, 3.5, 0.014
F(000)	1164	3088	3096	3112
Transm. ratio (max/min)	2.59	2.41	1.69	9.94
θ range (deg)	2–31	3–30	3–30	1–30
Range in *h k l*	±25, ±11, ±5	±31, ±6, ±23	±31, ±6, ±23	±30, ±5, ±22
Total no. reflections	5289	7058	6862	6433
Independent reflections	891 ($R_{int}=0.1115$)	2154 ($R_{int}=0.0550$)	2147 ($R_{int}=0.0273$)	2003 ($R_{int}=0.0833$)
Reflections with $I>2\sigma(I)$	422 ($R_\sigma=0.2192$)	1744 ($R_\sigma=0.0433$)	1810 ($R_\sigma=0.0242$)	876 ($R_\sigma=0.2263$)
Data/parameters	891/36	2154/108	2147/108	2003/109
Goodness-of-fit on F^2	0.473	1.098	1.082	0.501
Final *R* indices [$I>2\sigma(I)$]				
R_1	0.0282	0.0299	0.0205	0.0274
wR_2	0.0406	0.0667	0.0395	0.0497
R indices (all data)				
R_1	0.0871	0.0430	0.0301	0.0824
wR_2	0.0458	0.0794	0.0417	0.0550
Extinction coefficient	0.00176(7)	0.00067(4)	0.00035(1)	0.00056(1)
Largest diff. peak and hole ($e/Å^3$)	2.11/−2.93	3.05/–2.87	1.36/–2.39	1.64/–2.39

nickel/indium mixing, leading to the composition $Dy_4Ni_{10.80}In_{20.20}$ for the investigated single crystal. The final difference Fourier syntheses revealed no significant residual peaks for both refinements. The atomic parameters and interatomic distances are listed in Tables 2 and 3. Further data on the structure refinement are available.[1]

3.2. Crystal chemistry

New indides $Dy_5Ni_2In_4$, $Gd_4Ni_{11}In_{20}$, $Tb_4Ni_{11}In_{20}$, and $Dy_4Ni_{10.80}In_{20.20}$ have been synthesized from the elements and suitable single crystals for structure determination have been grown via special annealing sequences. In the series of $RE_5Ni_2In_4$ compounds (RE = Sc, Ho, Er, Tm, Lu [13,17]), $Dy_5Ni_2In_4$ is the representative with the largest rare earth element, and the course of this series seems to be limited at that size. The cell volume of $Dy_5Ni_2In_4$ is slightly larger than the volume of the holmium compounds as expected from the lanthanide contraction.

The monoclinic $U_4Ni_{11}Ga_{20}$ [14]/$Ho_4Ni_{10}Ga_{21}$ [21] type structure has so far only been observed for $Y_4Ni_{11}In_{20}$ [9]. We have now extended this series with the synthesis of $Gd_4Ni_{11}In_{20}$, $Tb_4Ni_{11}In_{20}$, and $Dy_4Ni_{10.80}In_{20.20}$. The cell volume of the yttrium compounds is the smallest one in the $RE_4Ni_{11}In_{20}$ series. The crystal chemistry of the $Lu_5Ni_2In_4$ [13] and $Ho_4Ni_{10}Ga_{21}$ [21] type compounds has been described in detail in previous work [9,14,19–24]. Herein, we focus only on the comparative structural description of $Dy_5Ni_2In_4$ and $Dy_4Ni_{10.80}In_{20.20}$.

A projection of the $Dy_5Ni_2In_4$ structure along the short unit cell axis is presented in Fig. 1. The nickel and indium atoms have trigonal prismatic and distorted square prismatic dysprosium coordination, respectively. Together, the nickel and indium atoms build up one-dimensional $[Ni_2In_4]$ polyanionic networks which extend in the *b* direction. These networks are embedded in a matrix of dysprosium atoms. Within the dysprosium matrix (trigonal and square prisms) we observe a broad range of Dy–Dy distances (338–379 pm). Compared with the average

[1]Details may be obtained from: Fachinformationszentrum Karlsruhe, D-76344 Eggenstein-Leopoldshafen (Germany), by quoting the Registry Nos. CSD–418923 ($Dy_5Ni_2In_4$), CSD–418922 ($Gd_4Ni_{11}In_{20}$), CSD–418921 ($Tb_4Ni_{11}In_{20}$), and CSD–418920 ($Dy_4Ni_{10.80}In_{20.20}$).

Table 2
Atomic coordinates and isotropic displacement parameters (pm^2) of $Dy_5Ni_2In_4$ and $RE_4Ni_{11}In_{20}$ (RE = Gd, Tb, Dy)

Atom	Wyckoff position	Occupancy (%)	x	y	z	U_{eq}
$Dy_5Ni_2In_4$ (space group Pbam)						
Dy_1	2*a*	100	0	0	0	68(3)
Dy_2	4*g*	100	0.22049(6)	0.24487(13)	0	85(2)
Dy_3	4*g*	100	0.41434(6)	0.11706(11)	0	63(2)
Ni	4*h*	100	0.30401(15)	0.0256(3)	1/2	78(6)
In_1	4*h*	100	0.56959(8)	0.20712(15)	1/2	76(3)
In_2	4*h*	100	0.84744(9)	0.07336(17)	1/2	82(3)
$Gd_4Ni_{11}In_{20}$ (space group C2/m)						
Gd_1	4*i*	100	0.11884(3)	0	0.33209(4)	73(1)
Gd_2	4*i*	100	0.77136(3)	0	0.17530(4)	76(1)
Ni_1	4*i*	100	0.02235(9)	0	0.59963(12)	91(3)
Ni_2	4*i*	100	0.13486(10)	0	0.10231(12)	97(3)
Ni_3	4*i*	100	0.25290(9)	0	0.61672(12)	85(3)
Ni_4	4*i*	100	0.34766(9)	0	0.12079(12)	98(3)
Ni_5	4*i*	100	0.50554(9)	0	0.19373(12)	87(3)
Ni_6	2*d*	100	0	1/2	1/2	103(5)
In_1	4*i*	100	0.00920(5)	0	0.09448(7)	91(2)
In_2	4*i*	100	0.06379(5)	0	0.79019(7)	80(2)
In_3	4*i*	100	0.11545(5)	0	0.55166(7)	99(2)
In_4	4*i*	100	0.20186(5)	0	0.00276(6)	76(2)
In_5	4*i*	100	0.24649(5)	0	0.29143(6)	72(2)
In_6	4*i*	100	0.29688(5)	0	0.49753(6)	72(2)
In_7	4*i*	100	0.38876(5)	0	0.30936(6)	85(2)
In_8	4*i*	100	0.39828(5)	0	0.00781(6)	82(2)
In_9	4*i*	100	0.54063(5)	0	0.37779(7)	85(2)
In_{10}	4*i*	100	0.62758(5)	0	0.19572(6)	76(2)
$Tb_4Ni_{11}In_{20}$ (space group C2/m)						
Tb_1	4*i*	100	0.11902(2)	0	0.33168(3)	70(1)
Tb_2	4*i*	100	0.77125(2)	0	0.17470(3)	73(1)
Ni_1	4*i*	100	0.02242(5)	0	0.59970(7)	90(2)
Ni_2	4*i*	100	0.13561(6)	0	0.10247(7)	92(2)
Ni_3	4*i*	100	0.25315(5)	0	0.61693(7)	81(2)
Ni_4	4*i*	100	0.34756(5)	0	0.12109(7)	87(2)
Ni_5	4*i*	100	0.50587(5)	0	0.19413(7)	85(2)
Ni_6	2*d*	100	0	1/2	1/2	89(3)
In_1	4*i*	100	0.00968(3)	0	0.09480(4)	83(1)
In_2	4*i*	100	0.06358(3)	0	0.79005(4)	76(1)
In_3	4*i*	100	0.11555(3)	0	0.55167(4)	93(1)
In_4	4*i*	100	0.20191(3)	0	0.00262(4)	69(1)
In_5	4*i*	100	0.24672(3)	0	0.29128(4)	69(1)
In_6	4*i*	100	0.29684(3)	0	0.49761(4)	68(1)
In_7	4*i*	100	0.38855(3)	0	0.30897(4)	81(1)
In_8	4*i*	100	0.39831(3)	0	0.00823(4)	75(1)
In_9	4*i*	100	0.54082(3)	0	0.37749(4)	79(1)
In_{10}	4*i*	100	0.62791(3)	0	0.19569(4)	71(1)
$Dy_4Ni_{10.80(3)}In_{20.20(3)}$ (space group C2/m)						
Dy_1	4*i*	100	0.11935(6)	0	0.33120(8)	66(3)
Dy_2	4*i*	100	0.77085(7)	0	0.17383(9)	72(3)
Ni_1	4*i*	100	0.02288(18)	0	0.6006(2)	79(6)
Ni_2	4*i*	100	0.13651(18)	0	0.1027(2)	76(7)
Ni_3	4*i*	100	0.25403(18)	0	0.6173(2)	75(7)
Ni_4	4*i*	100	0.34735(17)	0	0.1216(2)	70(7)
Ni_5	4*i*	100	0.50685(17)	0	0.1948(2)	75(7)
Ni_6/In_{11}	2*d*	80(3)/20(3)	0	1/2	1/2	151(18)
In_1	4*i*	100	0.01026(9)	0	0.09479(12)	79(4)
In_2	4*i*	100	0.06356(9)	0	0.79037(12)	72(3)
In_3	4*i*	100	0.11585(9)	0	0.55211(12)	72(4)
In_4	4*i*	100	0.20198(9)	0	0.00256(12)	65(4)
In_5	4*i*	100	0.24719(9)	0	0.29141(12)	59(4)
In_6	4*i*	100	0.29701(10)	0	0.49779(12)	56(4)
In_7	4*i*	100	0.38831(9)	0	0.30850(13)	76(4)
In_8	4*i*	100	0.39845(9)	0	0.00871(12)	61(4)
In_9	4*i*	100	0.54096(9)	0	0.37704(12)	75(4)
In_{10}	4*i*	100	0.62826(9)	0	0.19532(12)	68(4)

U_{eq} is defined as one third of the trace of the orthogonalized U_{ij} tensor.

Table 3
Interatomic distances (pm), calculated with the powder lattice parameters of $Dy_5Ni_2In_4$ and $Dy_4Ni_{10.80(3)}In_{20.20(3)}$

$Dy_5Ni_2In_4$										
Dy_1	4	In_1	317.8	Dy_3	2	Ni	276.3	In_1	1	Ni	290.7
	4	In_2	331.4		2	In_1	313.7		2	Dy_3	313.7
	2	Dy_3	338.2		2	In_2	325.7		2	Dy_1	317.8
	2	Dy_1	359.9		2	In_1	337.9		1	In_2	324.3
Dy_2	2	Ni	288.5		1	Dy_1	338.2		2	Dy_2	326.0
	2	Ni	290.5		1	Dy_3	357.0		2	Dy_3	337.9
	2	In_2	322.8		2	Dy_3	359.9		2	In_1	359.9
	2	In_1	326.0		1	Dy_2	360.2	In_2	1	Ni	281.2
	2	In_2	331.5		1	Dy_2	379.2		2	Dy_2	322.8
	2	Dy_2	359.9	Ni	2	Dy_3	276.3		1	In_1	324.3
	1	Dy_3	360.2		1	In_2	281.2		2	Ni	325.2
	1	Dy_3	379.2		2	Dy_2	288.5		1	Dy_3	325.7
					2	Dy_2	290.5		2	Dy_1	331.4
					1	In_1	290.7		2	Dy_2	331.5
					1	In_2	325.2				
					2	Ni	359.9				
$Dy_4Ni_{10.80(3)}In_{20.20(3)}$										
Dy_1	2	Ni_5	311.0	Ni_5	1	In_8	263.4	In_5	2	Ni_3	264.1
	2	In_9	313.9		1	In_9	266.5		1	Ni_2	267.6
	2	In_6	318.9		1	In_{10}	272.9		1	In_6	293.8
	2	In_{10}	320.6		2	In_1	274.6		1	In_7	302.6
	1	In_1	323.9		2	In_2	276.7		2	In_{10}	308.3
	2	Ni_3	327.6		1	Ni_4	307.0		2	Dy_2	314.8
	1	In_5	329.9		2	Dy_1	311.0		1	Dy_1	329.9
	1	In_6	333.1	Ni_6	4	Ni_1	259.1		2	In_3	343.5
	1	In_2	340.7		2	In_9	267.4	In_6	1	Ni_3	265.6
	1	In_3	371.2		2	In_7	271.2		2	Ni_3	266.7
Dy_2	2	In_5	314.8		4	In_3	310.3		1	In_5	293.8
	2	In_7	314.9	In_1	2	Ni_5	274.6		1	In_9	300.5
	2	Ni_4	317.0		1	Ni_2	277.1		2	In_6	305.0
	2	In_4	318.1		1	In_1	290.9		2	Dy_1	318.9
	1	In_8	325.6		2	In_8	298.9		2	In_3	331.9
	1	In_4	331.3		1	Ni_2	306.1		1	Dy_1	333.1
	2	Ni_2	333.6		2	In_{10}	307.4	In_7	1	Ni_4	268.8
	1	In_{10}	342.6		1	In_2	316.1		1	Ni_6	271.2
	1	In_2	342.7		1	Dy_1	323.9		2	Ni_1	273.6
	1	In_3	374.5	In_2	2	Ni_4	273.3		1	In_9	294.5
Ni_1	2	Ni_6	259.1		1	Ni_1	273.5		1	In_5	302.6
	1	In_3	263.6		2	Ni_5	276.7		2	Dy_2	314.9
	1	In_3	268.3		1	In_4	310.8		2	In_3	320.0
	2	In_9	272.9		1	In_1	316.1		2	In_2	324.4
	1	In_2	273.5		2	In_9	323.6	In_8	1	Ni_5	263.4
	2	In_7	273.6		2	In_7	324.4		2	Ni_2	265.0
	1	Ni_1	288.4		1	Dy_1	340.7		1	Ni_4	269.9
Ni_2	2	In_8	265.0		1	Dy_2	342.7		2	In_1	298.9
	1	In_5	267.6		2	In_8	364.0		2	In_4	305.1
	2	In_{10}	271.2	In_3	1	Ni_1	263.6		1	In_{10}	308.5
	1	In_1	277.1		1	Ni_3	265.2		1	Dy_2	325.6
	1	In_4	277.8		1	Ni_1	268.3		2	In_2	364.0
	1	In_1	306.1		2	Ni_6	310.3	In_9	1	Ni_5	266.5
	2	Dy_2	333.6		2	In_7	320.0		1	Ni_6	267.4
Ni_3	2	In_5	264.1		2	In_9	321.9		2	Ni_1	272.8
	1	In_3	265.2		2	In_6	331.9		1	In_7	294.5
	1	In_6	265.5		2	In_5	343.5		1	In_6	300.5
	2	In_6	266.7		1	Dy_1	371.2		2	Dy_1	313.9
	1	In_{10}	270.9		1	Dy_2	374.5		2	In_3	321.9
	2	Dy_1	327.6	In_4	1	Ni_4	269.8		2	In_2	323.6
Ni_4	1	In_7	268.8		2	Ni_4	274.2	In_{10}	1	Ni_3	270.9
	1	In_4	269.8		1	Ni_2	277.8		2	Ni_2	271.2
	1	In_8	269.9		2	In_8	305.1		1	Ni_5	272.9
	2	In_2	273.3		2	In_4	308.7		2	In_1	307.4
	2	In_4	274.2		1	In_2	310.8		2	In_5	308.3
	1	Ni_5	307.0		2	Dy_2	318.1		1	In_8	308.5
	2	Dy_2	317.0		1	Dy_2	331.3		2	Dy_1	320.6
									1	Dy_2	342.6

Standard deviations are all equal or smaller than 0.3 pm. All distances within the first coordination spheres are listed.

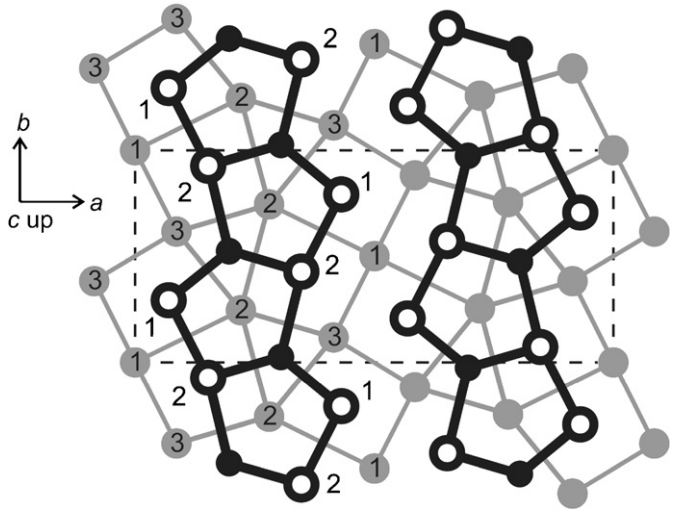

Fig. 1. Projection of the $Dy_5Ni_2In_4$ structure along the *c*-axis. Dysprosium, nickel, and indium atoms are drawn as medium grey, black filled, and open circles, respectively. The trigonal and square prismatic coordination of the nickel and indium atoms is emphasized. All atoms lie on mirror planes at $z = 0$ (thin lines) and $z = 1/2$ (thick lines).

Dy–Dy distance of 355 pm in *h c p* dysprosium [25], these contacts can be considered as bonding (Fig. 2).

Each nickel atom has three indium neighbours at Ni–In distances ranging from 281 to 325 pm, much longer than the sum of the covalent radii of 265 pm [26], indicating only weak Ni–In bonding in $Dy_5Ni_2In_4$. The shortest distances occur for Dy–Ni (289 and 291 pm), close to the sum of the covalent radii of 274 pm [26]. Certainly the Dy–Ni contacts significantly contribute to the stability of the structure.

A completely different bonding situation occurs in $Dy_4Ni_{10.80}In_{20.20}$. Here, the dysprosium atoms are the minority component, and they are embedded within the three-dimensional $[Ni_{10.80}In_{20.20}]$ polyanionic network. The latter shows strong Ni–Ni (259 pm), Ni–In (263–310 pm), and In–In (291–364 pm) bonding. The dysprosium atoms are well separated from each other. The shortest Dy–Dy contact corresponds to the *b* lattice parameter. Within the $[Ni_{10.80}In_{20.20}]$ network the indium atoms show the motif of slightly distorted *bcc* indium cubes, similar to the structure of tetragonal indium (4×325 and 8×338 pm) [25].

Three crystals of the monoclinic structure type have been investigated. Special care was taken with respect to the occupancy of the 2*d* position, which can either be occupied by a transition metal atom or a group III element, classifying the respective compound to the $U_4Ni_{11}Ga_{20}$ [14] or $Ho_4Ni_{10}Ga_{21}$ [21] type. The $Gd_4Ni_{11}In_{20}$ and $Tb_4Ni_{11}In_{20}$ crystals revealed full occupancy with nickel, while mixed Ni/In occupancy has been observed for $Dy_4Ni_{10.80}In_{20.20}$. In all $RE_4Pd_{10}In_{21}$ indides [19,27] the 2*d* site is exclusively occupied by indium, while the $RE_4Pt_{10}In_{21}$ indides [20] reveal some In/Pt mixing.

Summing up, the indides $Dy_5Ni_2In_4$ and $Dy_4Ni_{10.80}In_{20.20}$ reveal different bonding peculiarities depending on the dysprosium content, i.e. a one-dimensional $[Ni_2In_4]$ network and significant Dy–Dy bonding in

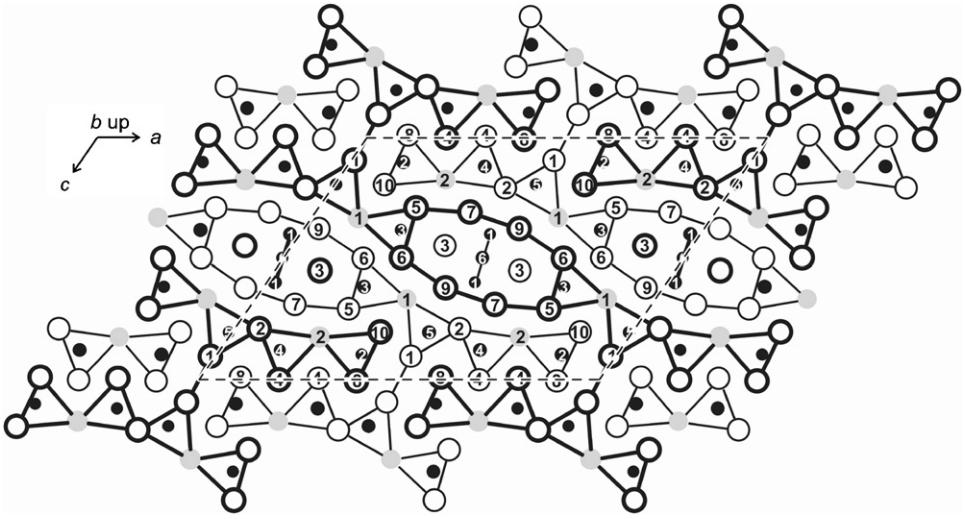

Fig. 2. Projection of the $Dy_4Ni_{10.80}In_{20.20}$ structure along the *b*-axis. Dysprosium, nickel, and indium atoms are drawn as medium grey, black filled, and open circles, respectively. The trigonal prismatic coordination of the nickel atoms is emphasized. Note that the Ni_6 position shows mixed Ni/In occupancy (see Table 2). Prisms drawn with thin and thick lines are shifted by half the translation period *b*.

$Dy_5Ni_2In_4$ and a covalently bonded three-dimensional $[Ni_{10.80}In_{20.20}]$ network with embedded, well-separated dysprosium atoms in $Dy_4Ni_{10.80}In_{20.20}$.

Acknowledgments

We are grateful to Dipl.-Chem. F.M. Schappacher for the work at the scanning electron microscope. This work was supported by the Deutsche Forschungsgemeinschaft. Yu.B. T. is indebted to the DAAD for a research stipend.

References

[1] Ya.M. Kalychak, V.I. Zaremba, R. Pöttgen, M. Lukachuk, R.-D. Hoffmann, Rare earth–transition metal–indides, in: K.A. Gschneider Jr., V.K. Pecharsky, J.-C. Bünzli (Eds.), Handbook on the Physics and Chemistry of Rare Earths, vol. 34, Elsevier, Amsterdam, 2005, pp. 1–133 (Chapter 218).
[2] K.H.J. Buschow, J. Less Common Met. 39 (1975) 185.
[3] J.W.C. de Vries, R.C. Thiel, K.H.J. Buschow, J. Less Common Met. 111 (1985) 313.
[4] H. Fujii, T. Inoue, Y. Andoh, T. Takabatake, Y. Satoh, Y. Maeno, T. Fujita, J. Sakurai, Y. Yamaguchi, Phys. Rev. B 39 (1989) 6840.
[5] B. Chevalier, M.L. Kahn, J.-L. Bobet, M. Pasturel, J. Etourneau, J. Phys. Condens. Matter 14 (2002) L365.
[6] Ya.M. Kalychak, P. Yu . Zavalij, V.M. Baranyak, O.V. Dmytrakh, O.I. Bodak, Kristallografiya 32 (1987) 1021.
[7] J. Tang, K.A. Gschneidner Jr., S.J. White, M.R. Roser, T.J. Goodwin, L.R. Corruccini, Phys. Rev. B 52 (1995) 7328.
[8] V.I. Zaremba, Ya.M. Kalychak, Yu.B. Tyvanchuk, R.-D. Hoffmann, M.H. Möller, R. Pöttgen, Z. Naturforsch. 57b (2002) 791.
[9] V. Hlukhyy, V.I. Zaremba, Ya.M. Kalychak, R. Pöttgen, J. Solid State Chem. 177 (2004) 1359.
[10] V.I. Zaremba, V. Hlukhyy, R. Pöttgen, Z. Anorg. Allg. Chem. 631 (2005) 327.
[11] V.I. Zaremba, I.R. Muts, U.Ch. Rodewald, V. Hlukhyy, R. Pöttgen, Z. Anorg. Allg. Chem. 630 (2004) 1903.
[12] M. Lukachuk, Ya.V. Galadzhun, R.I. Zaremba, M.V. Dzevenko, Ya.M. Kalychak, V.I. Zaremba, U.Ch. Rodewald, R. Pöttgen, J. Solid State Chem. 178 (2005) 2724.
[13] V.I. Zaremba, Ya.M. Kalychak, P.Yu. Zavalii, V.A. Bruskov, Kristallografiya 36 (1991) 1415.
[14] Yu.N. Grin, P. Rogl, J. Nucl. Mater. 137 (1986) 89.
[15] R. Pöttgen, Th. Gulden, A. Simon, GIT Labor Fachzeitschrift 43 (1999) 133.
[16] K. Yvon, W. Jeitschko, E. Parthé, J. Appl. Crystallogr. 10 (1977) 73.
[17] M. Lukachuk, B. Heying, U.Ch. Rodewald, R. Pöttgen, Heteroatom. Chem. 16 (2005) 364.
[18] G.M. Sheldrick, SHELXL-97, Program for Crystal Structure Refinement, University of Göttingen, Germany, 1997.
[19] V.I. Zaremba, U.Ch. Rodewald, Ya.M. Kalychak, Ya.V. Galadzhun, D. Kaczorowski, R.-D. Hoffmann, R. Pöttgen, Z. Anorg. Allg. Chem. 629 (2003) 434.
[20] V.I. Zaremba, V. Hlukhyy, U.Ch. Rodewald, R. Pöttgen, Z. Anorg. Allg. Chem. 631 (2005) 1371.
[21] Yu.N. Grin, Ya.P. Yarmolyuk, E.I. Gladyshevskii, Dokl. Akad. Nauk SSSR 245 (1979) 1102 (in Russian).
[22] M. Lukachuk, R.-D. Hoffmann, R. Pöttgen, Monatsh. Chem. 136 (2005) 127.
[23] R. Zaremba, U.Ch. Rodewald, R. Pöttgen, Monatsh. Chem. 138 (2007) 819.
[24] A.I. Tursina, Z.M. Kurenbaeva, D.V. Shtepa, S.N. Nesterenko, H. Noël, Acta Crystallogr. E 62 (2006) i80.
[25] J. Donohue, The Structures of the Elements, Wiley, New York, 1974.
[26] J. Emsley, The Elements, Oxford University Press, Oxford, 1999.
[27] K. Łątka, M. Rams, R. Kmieć, A.W. Pacyna, V.I. Zaremba, U.Ch. Rodewald, R. Pöttgen, Solid State Sci. 9 (2007) 173.